

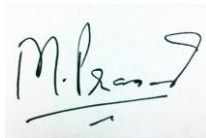
DOE Award No.: DE-FE-0009963

Quarterly Research Performance Progress Report (Period ending 09/30/2016)

Measurement and Interpretation of Seismic Velocities and Attenuations in Hydrate-Bearing Sediments

Project Period (10/1/2012 to 12/31/2016)

Submitted by:
co-PI: Manika Prasad
Colorado School of Mines
DUNS #010628170.
1500 Illinois Street
Golden, CO 80401
e-mail: mprasad@mines.edu
Phone number: (303) 273-3457
Submission Date: 10/31/2016



Prepared for:
United States Department of Energy
National Energy Technology Laboratory



Office of Fossil Energy

Disclaimer

This report was prepared as an account of work sponsored by an agency of the United States Government. Neither the United States Government nor any agency thereof, nor any of their employees, makes any warranty, express or implied, or assumes any legal liability or responsibility for the accuracy, completeness, or usefulness of any information, apparatus, product, or process disclosed, or represents that its use would not infringe privately owned rights. Reference herein to any specific commercial product, process, or service by trade name, trademark, manufacturer, or otherwise does not necessarily constitute or imply its endorsement, recommendation, or favoring by the United States Government or any agency thereof. The views and opinions of authors expressed herein do not necessarily state or reflect those of the United States Government or any agency thereof.

Abstract

Measurement and Interpretation of Seismic Velocities and Attenuations in Hydrate-Bearing Sediments

Grant/Cooperative Agreement DE-FE 0009963.

During this quarter, we analyzed ultrasonic velocity measurements of pure sand packs and sand packs mixed with clay with regard to their ultrasonic attenuation. The attenuation analysis shows that the clay initially causes an increase in P-wave attenuation, Q_p^{-1} but after hydrate formation and dissociation these values are comparable to the values of our measurements for pure quartz sand. This observation leads to the assumption that after hydrate formation, clay grains are either pushed closer to the quartz grains and/or the clay grains are compressed into smaller aggregates. The observed attenuation values after hydrate formation show no influence with respect to the presence of clay but shows a distinct change in the loss mechanisms. A comparison of our ultrasonic attenuation measurements with well log data shows an overlap between the two data sets. We are now compiling seismic attenuation data to investigate if the loss mechanisms are independent of frequency over the full frequency range.

We updated the micro CT pressure and temperature control system by including a feed-through for fluid lines and wires and ultrasonic P-wave transducers. The experimental setup has been pressure tested for pressures up to 5000 psi (35 MPa) and is ready to be used for the formation of methane hydrate in the micro CT machine.

Table of Contents

Disclaimer	1
Abstract	3
Table of Contents.....	4
List of Figures and Tables	5
<i>List of Figures</i>	<i>5</i>
<i>List of Tables</i>	<i>5</i>
2. Accomplishments.....	6
2.1 Overview of Milestone Status.....	6
2.2 Ultrasonic Attenuation of Clay Filled Sand Packs before and after Hydrate Formation	8
2.3 Updates of Pressure and Temperature Control System in Micro CT	14
3. Acknowledgments.....	18
4. Plans	19
5. Products.....	20
6. Participants and Collaborating Organizations.....	21
7. Changes / Problems	23
8. Special Reporting Requirements	24
9. Budgetary Information.....	25

List of Figures and Tables

List of Figures

Figure 1: Milestone Status. We are at the end of our 16th quarter and in the final phase of this project. In February 2016, we requested and were granted a no-cost extension until December 31, 2016.	6
Figure 2: Micro X-Ray CT images of dry Ottawa Sand with 0 (a), 10 (b), and 30 wt% (c) kaolinite.....	9
Figure 3: a) Normalized frequency content of a p-wave (blue) and aluminum standard (green), b) ratio between frequency content of aluminum and sample, the slope between the two black bars is γ	10
Figure 4: $1/Q_s$ vs. $1/Q_p$ for sand packs with 0 wt.% clay (a), 10 wt.% clay (b), and 30 wt.% clay (c). Black symbols are attenuation values before hydrate formation, Blue symbols are attenuation values with hydrates present in the sample, and Red symbols are attenuation values after hydrates were dissociated.	12
Figure 5: Loss diagram for our measurements before hydrate formation (black symbols), while hydrates are present in the sample (blue symbols), and for the samples after hydrates are dissociated. Squares are pure sand samples, circles are samples containing 10 wt.% clay, and triangles are samples containing 30 wt.% of clay. Yellow triangle is calculated using Guerin and Goldbergs (2002) equations obtained from well log field data for 80% hydrate saturation.....	13
Figure 6: Ultrasonic P-wave transducers for use in micro CT setup. A 4-mm-diameter PZT crystal is encased in a PEEK housing with 10 mm diameter. A pore fluid line is included in one of the transducers	14
Figure 7: Feed-through with 2 fluid lines, 4 wires and a thermocouple	15
Figure 8: Waveform (P-wave) collected for 102.1 mm aluminum standard	16
Figure 9: Castlegate sandstone sample between 2 ultrasonic transducers, covered with heat shrink tubing, connected to feed-through.....	16
Figure 10: Micro CT images of Castlegate sandstone at atmospheric pressure (left), 2000 psi (middle) and 4000 psi (right). We observed a reduction in porosity but no grain damage (resolution: 5 microns)	17

List of Tables

Table 1: Milestone status	7
Table 2: Q15 Milestones and Deliverables.....	19

2. Accomplishments

2.1 Overview of Milestone Status

Our current position is shown in the time chart in

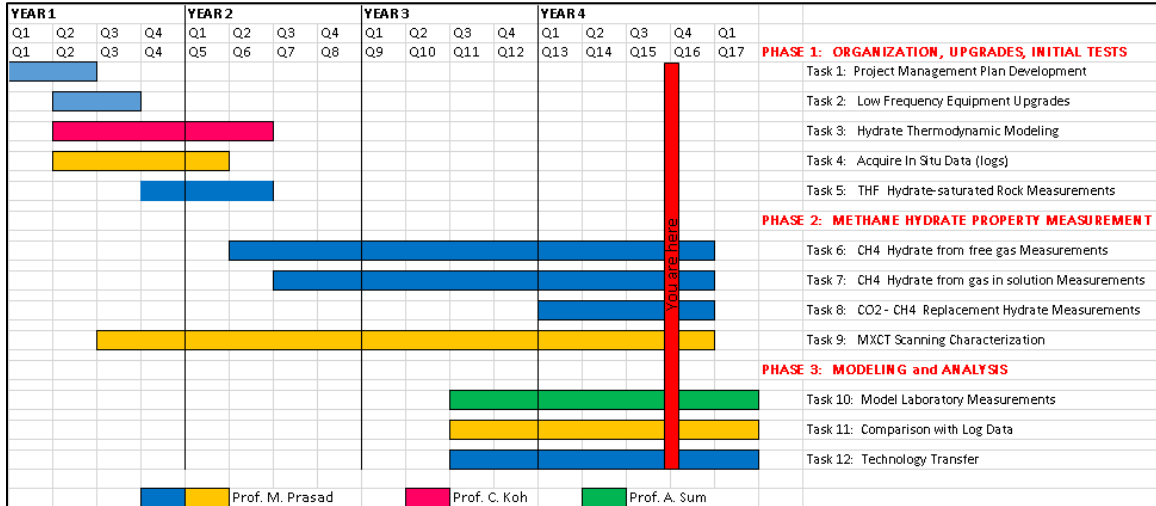


Figure 1 and the Milestone status is shown in Table 1. Note that we have been granted a no-cost extension until December 31, 2016. In the current period of Q16 (Q4 of Year 4), we continued our work on Task 9 – MXCT Characterization and Task 11 – Comparison with Log Data.

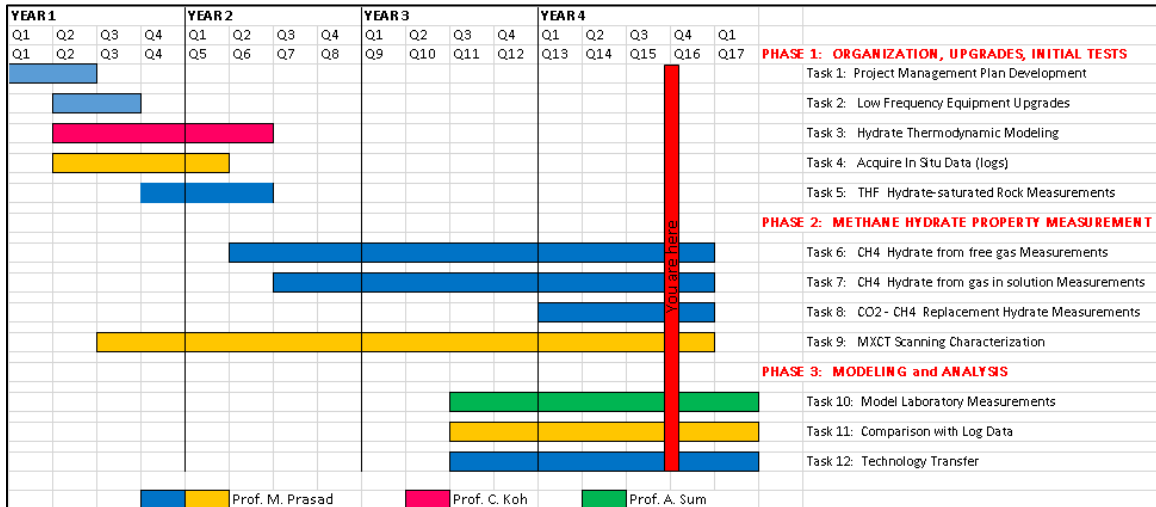


Figure 1: Milestone Status. We are at the end of our 16th quarter and in the final phase of this project. In February 2016, we requested and were granted a no-cost extension until December 31, 2016.

Table 1: Milestone status

Milestone	Title / Description	Status	Date: expected completed or)
Completed			
PHASE 1: ORGANIZATION, UPGRADES, INITIAL TESTS			
Task 1	Project Management Plan Development	Complete & approved	1-Dec-12
Task 2	Low Frequency Equipment Upgrades	Completed	1-Jun-13
Task 3	Hydrate Thermodynamic Modeling	Completed	31-May-14
Task 4	Acquire In Situ Data (logs)	Completed	31-May-14
Task 5	THF hydrate-saturated Rock measurement	Completed	15-Jun-14
Task 6	THF hydrate grown in pressure vessel	Completed	15-Apr-14
Continuing or Planned			
Task 7	CH4 hydrate from free gas Measurements	Continuing*	1-Oct-16
Task 8	CH4 hydrate (gas in solution) measurement	Planned	31-Oct-16
Task 9	CO2-CH4 replacement hydrate measurement	Planned	30-Nov-16
Task 10	MXCT Scanning Characterization	Continuing*	30-Nov-16
Task 11	Model Laboratory Measurements	Continuing*	30-Nov-16
Task 12	Comparison with Log Data	Continuing	30-Nov-16
Task 13	Technology Transfer	Continuing*	31-Dec-16
* initial stages were completed on schedule, but the process continues throughout the project			

2.2 Ultrasonic Attenuation of Clay Filled Sand Packs before and after Hydrate Formation

Experiment set up and procedures

For sample preparation, we thoroughly mixed Ottawa Sand F110 (pure quartz sand with 60-280 μm grain size) with a designated amount (0, 10, or 30 wt.%) of kaolinite, a non-swelling clay (Krishna et al., 1993), in a plastic container until the mixture visually appeared to be homogenous. Kaolinite was chosen because it showed the least swelling effects when in contact with water. This results in a texture in which clays will be dispersed and will structurally support some of the load on the frame (see microstructural details from microCT images shown in Figure 2). 16.1 g of the sand-clay mixture was placed into an instrumented sample holder and compacted to a designated volume (2.54 cm diameter, about 2.00 cm length). Exact sample length was measured using X-ray CT scans. The instrumented sample holder was comprised of PEEK (polyether ether ketone) end caps (1-inch diameter) surrounded by Tygon tubing. The end caps contained 500 kHz piezoelectric transducers as well as fluid lines for fluid injection and pore pressure control.

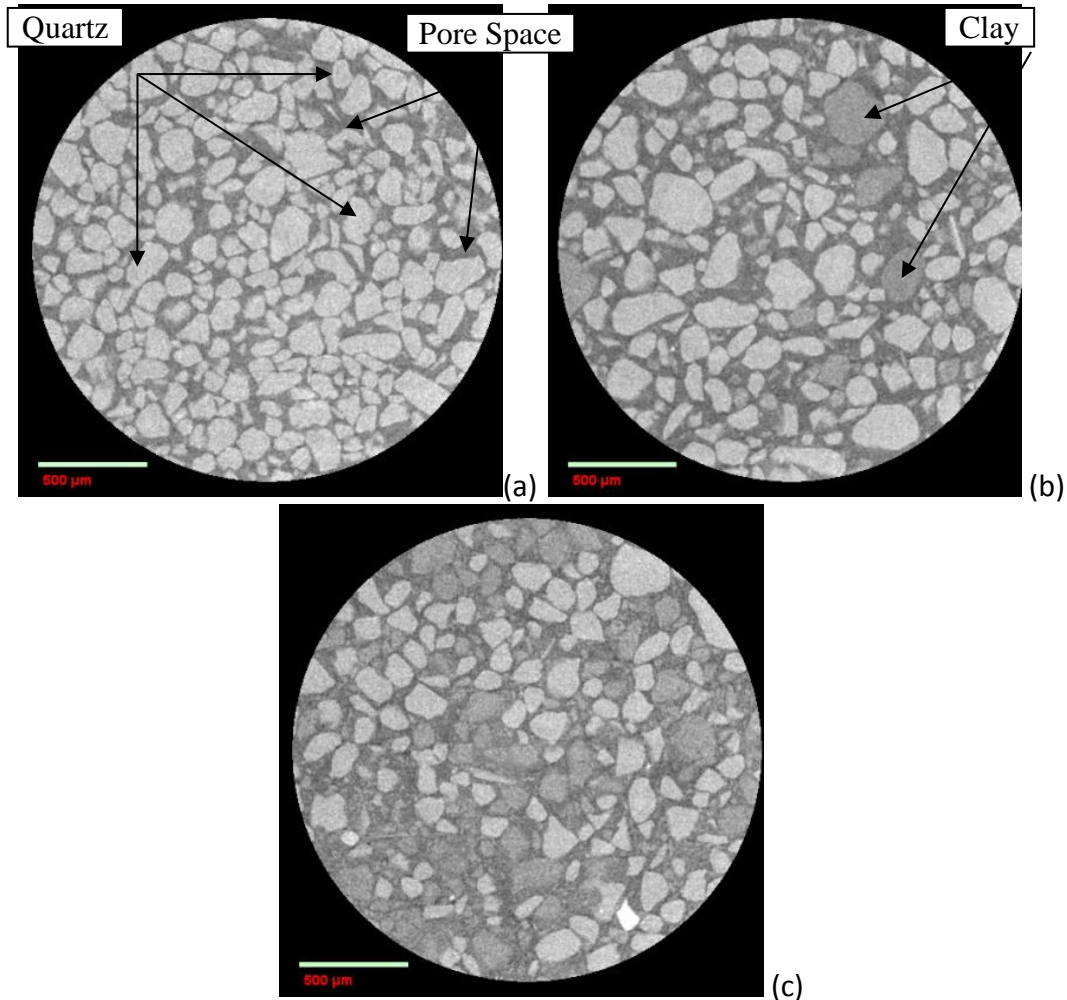


Figure 2: Micro X-Ray CT images of dry Ottawa Sand with 0 (a), 10 (b), and 30 wt% (c) kaolinite

The sample was submersed inside a temperature-controlled pressure vessel filled with hydraulic oil that allowed the application of a hydrostatic confining pressure. Two thermocouples were attached along the jacketed sample and recorded temperatures inside the pressure vessel. The sample was subjected to a confining pressure (P_c) of 535 psi (~ 3.7 MPa). After applying vacuum, a THF – H₂O solution, prepared such that it would yield 80% THF hydrate with residual water, was injected into the sample. Pore pressure (P_p) was kept constant at 100 psi (~ 0.7 MPa) resulting in a differential pressure (P_d) of 435 psi (~ 3 MPa). The pressure vessel temperature was then decreased from room temperature (~ 24 °C) down to ~ 1 °C at an average cooling rate of 6.5 °C/h. Ultrasonic p- and s-waves as well as temperature were recorded at regular intervals. The resulting ultrasonic velocities were calculated by dividing the sample length by the travel time of the first break picked from each waveform. Final measured velocity had to be corrected for the time the signal needed to go through the PEEK end caps (dead time correction). P- and s-wave velocities could be determined with an error of about 3.5 %. The main source for this error was the uncertainty in picking the correct arrival time. Additionally, we calculated the porosity based on the weight and volumetric dimensions of each specimen prior to hydrate formation. For each composition, the

velocities and porosity were measured in at least three samples prepared in the same way to establish degree of repeatability.

Ultrasonic Attenuation

The first cycle of the p-wave arrival was also analyzed for its frequency content using Fast Fourier transform. Ultrasonic attenuation was calculated with the spectral ratio method (Toksöz et al., 1978). Briefly, the amplitude spectrum of the first cycle of a waveform propagating through the sample is divided by a similar wave propagating through a standard sample. Aluminum was used as a standard material in this study. Both, the sample and the standard, were measured with the same transducers and had the same geometry. The slope of the frequency spectra ratio (Figure 3) is related to the quality factor Q (inverse of attenuation, Q^{-1}) by:

$$Q = \frac{\pi * l}{\gamma * v} \quad (1),$$

where Q is the quality factor [unitless], l is the length of the samples [in m], γ is the slope of the frequency ratios [in s], and v is the measured velocity [in m/s].

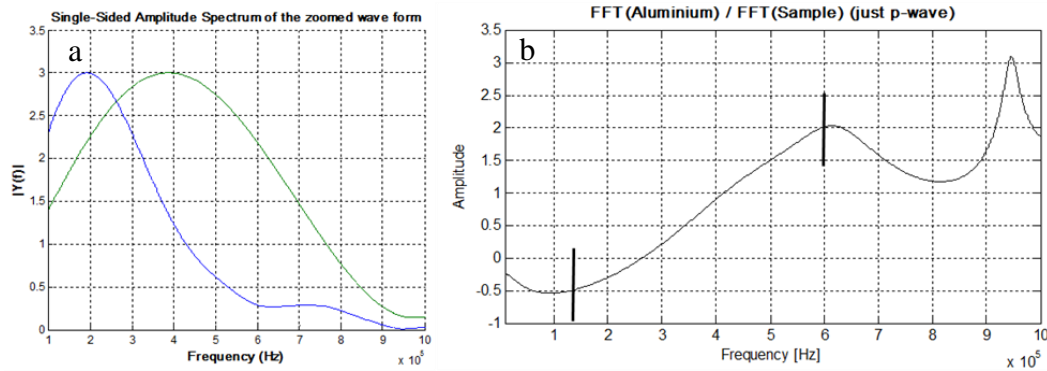


Figure 3: a) Normalized frequency content of a p-wave (blue) and aluminum standard (green), b) ratio between frequency content of aluminum and sample, the slope between the two black bars is γ .

Results:

Figure 4 shows the calculated attenuation values for (a) the sand packs without clay, the sand packs with 10 wt.% clay, and (c) the sand packs with 30 wt.% clay content. The $1/Q_p$ plot in Figure 4 show a marked difference in attenuation between the original sediment (black symbols) and in the sediment after hydrate dissociation (red symbols): Attenuation is greatly reduced in the sediment after hydrate dissociation as compared to attenuation in the sand pack sample before hydrate formation. This reduction in attenuation can be explained by the compaction process that occurred during the applied pressure cycle. This compaction was also noticeable in the compressional velocities which were slightly higher after than before hydrate formation. $1/Q_p$ increases with increasing clay content (Figure 4 b and c) before hydrate formation (black symbols) and it reaches values of around 3 for the samples with 30 wt.% clay. However, after dissociation, the attenuation values drastically reduce to values between 0.2 and 0.3. A possible explanation could be that the compliant clay particles are

present as grains alongside quartz sand in the mixed samples (Figure 2). Hydrate formation is accompanied by a volumetric expansion of around 7% (Lee et al., 2007). This volumetric expansion could cause a collapse of the compliant clay aggregate grains to a denser aggregate or push the clay aggregates against the quartz grains resulting in a stronger quartz – clay grain contact.

The attenuation values for the samples containing hydrates seem to be independent of the presence of clay. However, $1/Q_p$ and $1/Q_s$ are observed to increase with the presence of hydrates. As we have reported in the past, the hydrate itself has only a minimal attenuation; we have also reported that small amounts of free water can cause a drastic increase in attenuation. We make the same observation in our new experiments: After forming 80 % hydrate in the available pore space, the effective porosity is being reduced to 20 % of its original value. Additionally, the pore throat size is also being reduced and, in some cases, being potentially plugged. This could cause an increase in attenuation due to squirt flow as well as attenuation caused by scattering from pores that might be isolated and contain residual water.

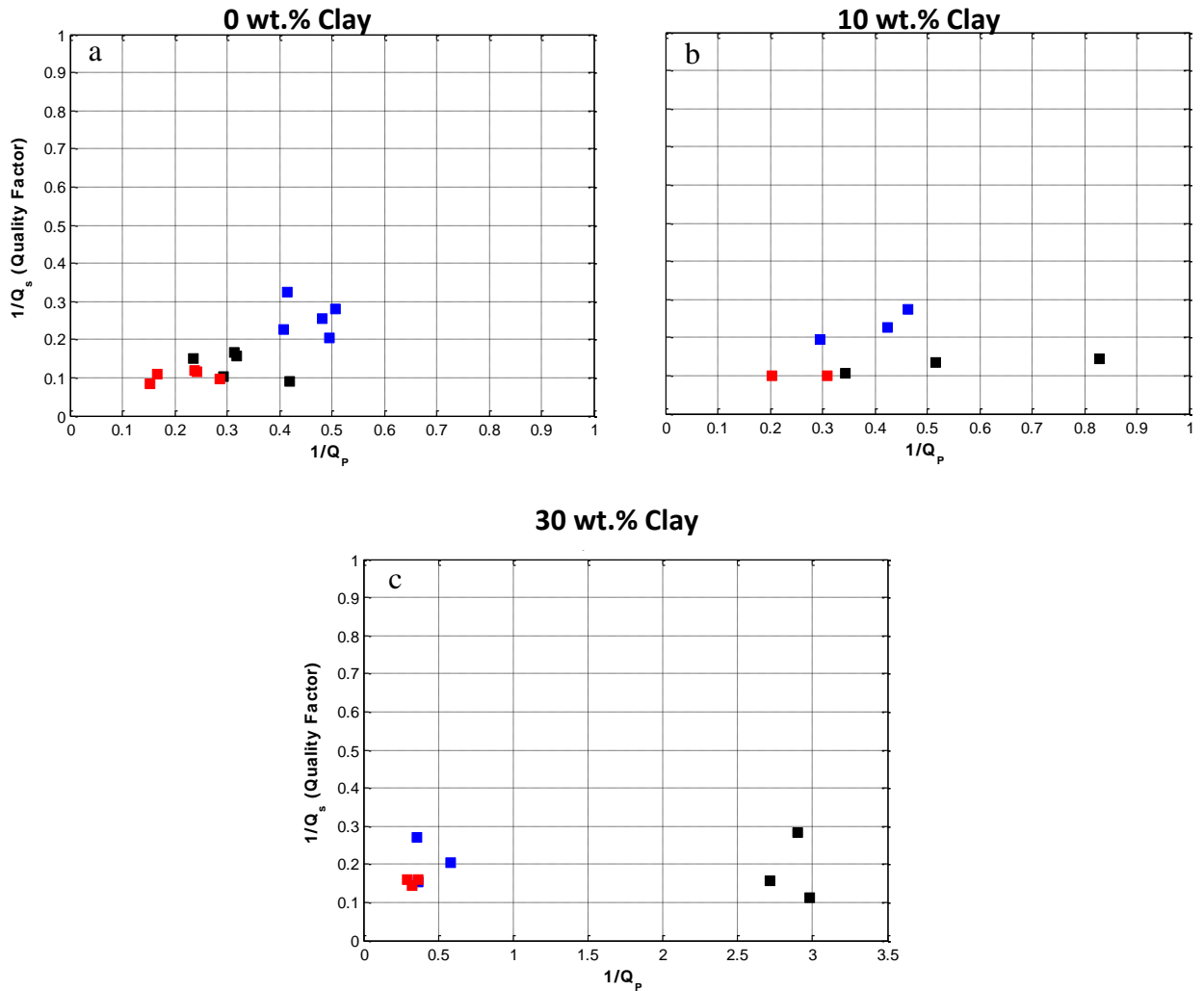


Figure 4: $1/Q_s$ vs. $1/Q_p$ for sand packs with 0 wt.% clay (a), 10 wt.% clay (b), and 30 wt.% clay (c). Black symbols are attenuation values before hydrate formation, Blue symbols are attenuation values with hydrates present in the sample, and Red symbols are attenuation values after hydrates were dissociated.

Loss Diagram:

Winkler and Nur (1982) demonstrated that by plotting (Q_p/Q_s) versus (V_p^2/V_s^2) , we are able to determine whether the losses are caused by the shear or the bulk losses in the sample. Figure 5 shows such a diagram for our measured data. All the samples that contained hydrates fall into a specific area characterized by high shear losses whereas the samples without hydrates cluster in a location where bulk losses are much larger than shear losses. In general, the S-wave velocities are strongly reduced by the presence of a fluid and therefore higher V_p - V_s ratios are expected and observed in our experimental data. In dry sediments, the V_p - V_s ratio is shifted to lower values. Our measurements with hydrates show the same behavior as dry samples. Even though the sample still contains residual water, the cementing effect caused by the hydrates overcomes the loss in shear strength caused by the presence of a liquid. We also compared our hydrate values with a value that can be obtained from the equations

provided by Guerin and Goldberg (2002) (Figure 5). They evaluated sonic well log data and calculated a linear regression for P- and S-wave velocities as well as for $1/Q_p$ and $1/Q_s$.

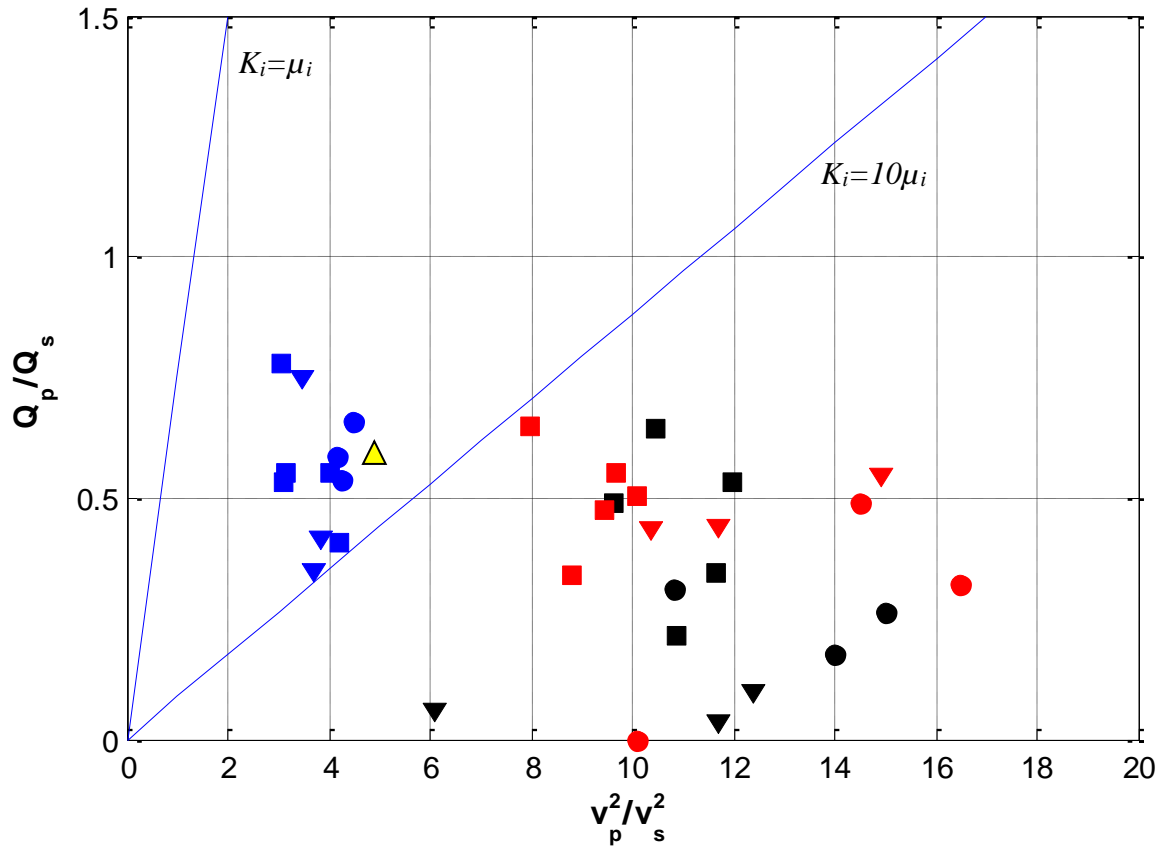


Figure 5: Loss diagram for our measurements before hydrate formation (black symbols), while hydrates are present in the sample (blue symbols), and for the samples after hydrates are dissociated. Squares are pure sand samples, circles are samples containing 10 wt.% clay, and triangles are samples containing 30 wt.% of clay. Yellow triangle is calculated using Guerin and Goldbergs (2002) equations obtained from well log field data for 80% hydrate saturation.

Conclusion

Initially, the presence of clay causes a drastic increase in $1/Q_p$ but after hydrate dissociation, $1/Q_p$ reduces to values comparable to $1/Q_p$ observed in pure quartz samples. After hydrate formation, the clay grains appear to have collapsed or pushed against the quartz grains. All samples containing hydrates cluster in the same area in the loss diagram and show similar values as dry sand samples. Comparing our results for the hydrate bearing sand packs with well log data shows a great agreement.

2.3 Updates of Pressure and Temperature Control System in Micro CT

We recently finished the assembly of a set of ultrasonic P-wave transducers (Figure 6) and a feed-through with 4 wires, a thermocouple and 2 fluid lines (Figure 7). The transducers consist of piezoelectric PZT P-wave crystals with a diameter of 4 mm encased by cylindrical pieces of PEEK. The PZT crystal is backed by a mixture of tungsten and epoxy to attenuate reflections from the back of the crystal. The ground wire is attached to the side of the PZT crystal facing towards the sample and is covered with a layer of conductive epoxy. The signal wire is attached to the back of the PZT crystal and held in place by the tungsten backing. To avoid pressure leak along the wires, we fixed them with ports at the outward facing end of the transducers and soldered wires to connect to the feed-through to the ports. The small dimensions of the transducers led us to the decision to initially include only P-wave crystals. A pore fluid line is added to one of the transducers. A hole is drilled through the entire length of the PEEK housing; the diameter of the hole is larger for the last 5 mm (1 mm diameter) to fit a stainless steel fluid line. The fluid line can be connected to the feed-through pore fluid line with a Swagelok fitting. The fluid line, ports and wires are protected and sealed by a layer of flexible epoxy on the outward facing side of the transducer.

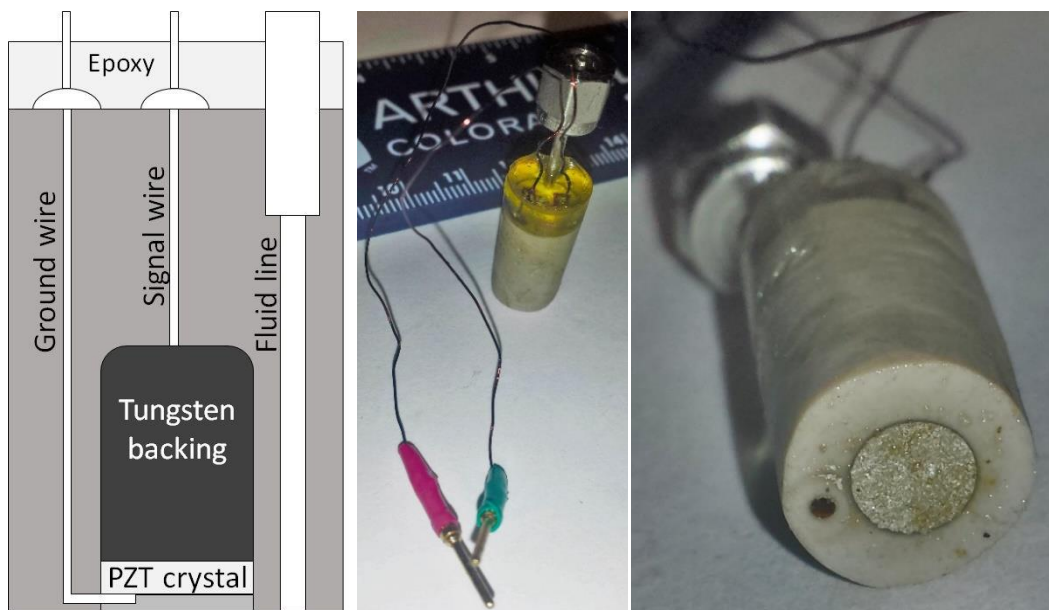


Figure 6: Ultrasonic P-wave transducers for use in micro CT setup. A 4-mm-diameter PZT crystal is encased in a PEEK housing with 10 mm diameter. A pore fluid line is included in one of the transducers

The feed-through is made of Torlon and can be connected to the CT pressure vessel with a Swagelok fitting. 8 holes were drilled through the Torlon cylinder – 4 for wires (a signal and a ground wire for each transducer), 2 for the two parts of a thermocouple and 2 for fluid lines. The pore fluid line has a Swagelok fitting to connect to the transducer, the confining pressure line is open on the inside of the cell due to confined

space but can be closed off with a Swagelok fitting on the outside of the cell. Top and bottom of the feed-through are sealed with flexible epoxy. A pressure test has shown that the feed-through is sealing the pressure cell for pressures up to 5000 psi for extended periods of time (testing time approximately 8 hours).

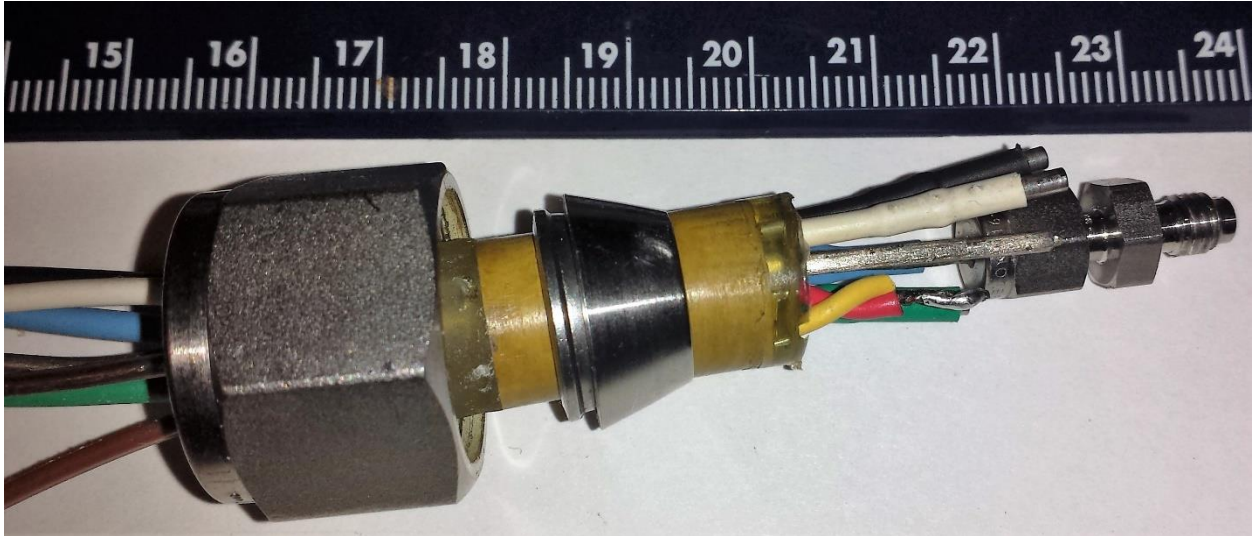


Figure 7: Feed-through with 2 fluid lines, 4 wires and a thermocouple

An example for a compressional waveform collected with the transducers is shown in Figure 8. The waveform was collected on a 102.1 mm long piece of aluminum at 22°C and atmospheric pressure. The dead time was estimated at $t_d = 1.01 \cdot 10^{-6} \text{ s}$, the travel time through the aluminum standard was $t = 1.679 \cdot 10^{-5} \text{ s}$, resulting in a velocity of $v_p = 6460 \text{ m/s}$. The P-wave first arrival has an amplitude of 25 mV proving that we will be able to obtain sufficient signal quality to reliably pick first arrival times in sediments.

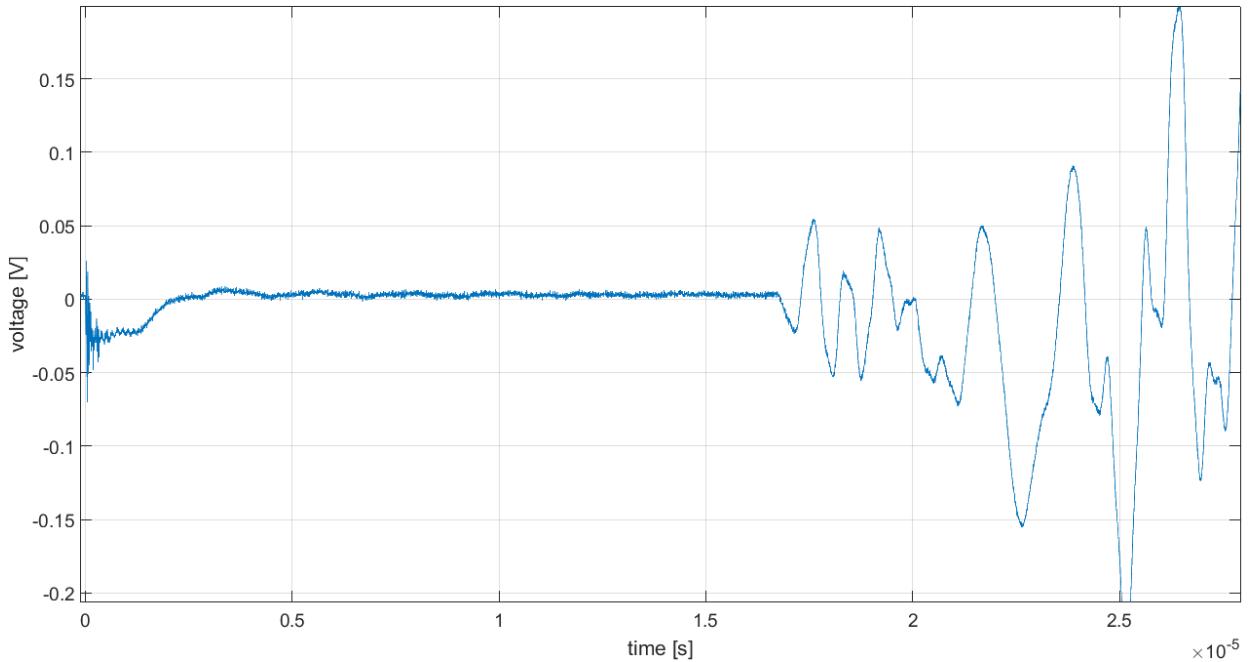


Figure 8: Waveform (P-wave) collected for 102.1 mm aluminum standard

Figure 9 shows a 15 mm long piece of Castlegate sandstone between the transducers. The sample is sealed with heat-shrink tubing and connected to the feed-through with the fluid line and the 2 ground wires and 2 signal wires.

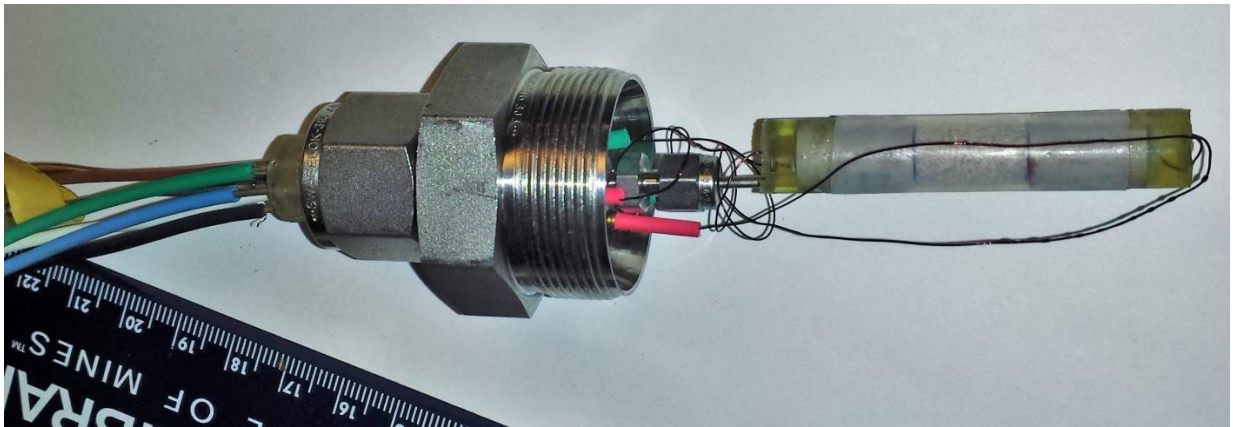


Figure 9: Castlegate sandstone sample between 2 ultrasonic transducers, covered with heat shrink tubing, connected to feed-through

The Castlegate sandstone sample was pressurized to confining pressures of 2000 psi (13.8 MPa) and 4000 psi (27.6 MPa). Micro CT images at atmospheric pressures, 2000 psi and 4000 psi are shown in Figure 10. The images are preliminary and will be repeated at better resolution and longer scanning duration to decrease the noise level. Figure 10 shows a compaction of the sample and a decrease of porosity with increasing confining pressure. These images prove that within our resolution limitations we will

be able to observe changes in the pore space, such as hydrate distribution and saturation.

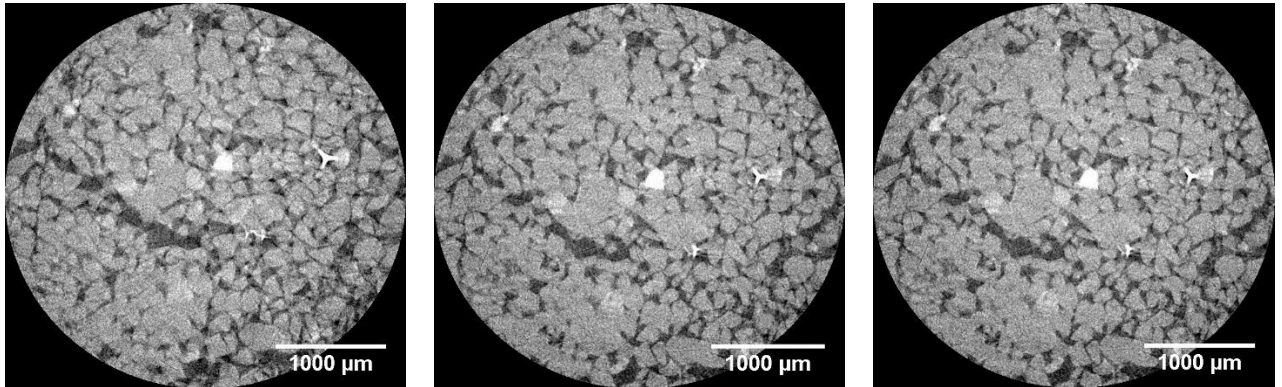


Figure 10: Micro CT images of Castlegate sandstone at atmospheric pressure (left), 2000 psi (middle) and 4000 psi (right). We observed a reduction in porosity but no grain damage (resolution: 5 microns)

The pressure and temperature control system in combination with ultrasonic transducers now allow us to form methane hydrates and to image hydrate distribution in rocks while simultaneously identifying their influence on ultrasonic velocities.

Our next step will be to (1) make microCT images and acoustic velocity measurements during methane hydrate formation, and (2) build transducers with P- and S-wave PZT crystals to conduct the same experiments as in (1) but with P- and S-wave measurements.

3. Acknowledgments

This project is funded by the U.S. Department of Energy (DOE) National Energy Technology Laboratory (NETL) under Grant Number DEFE0009963. This project is managed and administered by the Colorado School of Mines and funded by DOE/NETL and cost-sharing partners.

We thank the US Department of Energy for sponsoring the project. We also thank Tim Collett for his cooperation with us on this project. We acknowledge support of some personnel by other grants (DHI/Fluids and OCLASSH consortia).

References

- Guerin, G., and Goldberg, D., 2002. Sonic waveform attenuation in gas hydrate-bearing sediments from the Mallik 2L-38 research well, MacKenzie Delta, Canada. *J. Geophys. Res.*, 107:2088. doi:10.1029/2001JB000556
- Krishna K. Mohan, Ravimadhav N. Vaidya, Marion G. Reed, H. Scott Fogler, (1993), "Water sensitivity of sandstones containing swelling and non-swelling clays", *Colloids and Surfaces A: Physicochemical and engineering Aspects*. 73 (1993) 237-254
- Lee, J. Y., Yun, T. S., Santamarina, J. C., Ruppel, C. (2007). "Observations Related to Tetrahydrofuran and Methane Hydrates for Laboratory Studies of Hydrate-Bearing Sediments" *Geochemistry Geophysics Geosystems An Electronic Journal of the Earth Sciences*, 8 (6)
- Toksöz, M.N., Johnston, D.H., and Timur, A., (1978), Attenuation of seismic waves in dry and saturated rocks: 1. Laboratory measurement; *Geophysics*, 44, 681-690.
- Winkler, K. W., and Nur, 1982, Seismic attenuation: Effects of pore fluids and frictional sliding; *Geophysics*, 47, no. 1, 1-15.

4. Plans

Table 4 shows the Milestones and Deliverables for this quarter. We plan to focus on CH₄ hydrates in MXCT scanning. We are delayed in Milestone 7. Due to various delays in our experimentation and initial attempts failing to form methane out of the free gas phase, we anticipate a more realistic completion date of 12/31/2016. We needed to improve our experimental setup for P- and S-wave measurements due to leaks and poor signal quality. We plan to continue these measurements for the remaining samples. In addition to methane hydrate experiments, we will also perform methane – CO₂ exchange experiments to study their effects on acoustic, elastic, and attenuation properties.

We plan to extend our comparison of our attenuation results for sand packs with and without clay with more field data as well as with laboratory for methane hydrate bearing and ice bearing sand samples.

We are planning on performing MXCT measurements with our newly designed and tested feed-throughs to visually and acoustically observe methane hydrate formation in sediment out of the free gas phase. Further, we plan to compare our measured ultrasonic velocities with effective medium models and numerical finite difference models based on the micro CT images.

Table 2: Q15 Milestones and Deliverables

Milestone	Task	Description	Completion date	Report Content
7	6	Methane hydrates from free gas phase (delayed)	12/31/2016	Progress report
10	9	NMR/MXCT characterization	11/30/2016	Progress report
12	11	Comparison with Log Data	11/30/2016	Progress report
13	12	Information Dissemination	12/31/2016	Progress report

5. Products

Publications (Publications; Conference Papers, Presentations, Books)

Website or other Internet sites

<http://crusher.mines.edu/CRA-DOE-Hydrates>

Technologies or techniques

Nothing to report

Inventions, patent applications and/or licenses

Nothing to report

Other Products

Nothing to report

6. Participants and Collaborating Organizations

CSM personnel:

Name:	Manika Prasad
Project Role:	Principle Investigator
Nearest person month worked this period:	0.25
Contribution to Project:	Dr. Prasad helped with acoustic and attenuation measurements.
Additional Funding Support:	Academic faculty
Collaborated with individual in foreign country:	No
Country(ies) of foreign collaborator:	N/A
Travelled to foreign country:	Yes
If traveled to foreign country(ies),	India, Norway, Germany, Houston
Duration of stay:	1 months

Name:	Michael Batzle †
Project Role:	Principle Investigator
Nearest person month worked this period:	0
Contribution to Project:	Dr. Batzle was responsible for the overall (dis)organization of the project.
Additional Funding Support:	Academic faculty
Collaborated with individual in foreign country:	No
Country(ies) of foreign collaborator:	N/A
Travelled to foreign country:	No
If traveled to foreign country(ies),	N/A
Duration of stay:	N/A

Name:	Carolyn Koh
Project Role:	Co-Investigator
Nearest person month worked this period:	0.25
Contribution to Project:	Dr. Koh helped with CH ₄ hydrate experimental setup and measurements
Additional Funding Support:	Academic faculty
Collaborated with individual in foreign country:	No
Country(ies) of foreign collaborator:	N/A
Travelled to foreign country:	No
If traveled to foreign country(ies),	N/A
Duration of stay:	N/A

Name:	Weiping Wang
Project Role:	Laboratory Manager

Nearest person month worked this period:	1
Contribution to Project:	Mr. Wang assisted in equipment fabrication
Additional Funding Support:	DHI/Fluids consortium; DOE-CO2 project
Collaborated with individual in foreign country:	No
Country(ies) of foreign collaborator:	N/A
Travelled to foreign country:	No
If traveled to foreign country(ies):	N/A
duration of stay: N/A:	N/A

Name:	Mathias Pohl
Project Role:	Ph.D. student
Nearest person month worked this period:	3
Contribution to Project:	Mr. Pohl pressure tested new equipment and performed ultrasonic attenuation measurements.
Additional Funding Support:	N/A
Collaborated with individual in foreign country:	No
Country(ies) of foreign collaborator:	N/A
Travelled to foreign country:	No
If traveled to foreign country(ies)	N/A
duration of stay:	N/A

Name:	Mandy Schindler
Project Role:	Ph.D. student
Nearest person month worked this period:	3
Contribution to Project:	Ms. Schindler updated equipment for MX-CT scanner.
Additional Funding Support:	N/A
Collaborated with individual in foreign country:	No
Country(ies) of foreign collaborator:	N/A
Travelled to foreign country:	
If traveled to foreign country(ies),	N/A
duration of stay:	3 weeks

External Collaborations:

Dr. Tim Collett
 US Geologic Survey
 Denver, Colorado

Support: Dr. T. Collett provided data and guidance on interpretation and application. He continues to publish numerous papers on hydrate properties.

7. Changes / Problems

We requested and were granted a no-cost extension until December 31, 2016. The extension was necessitated due to delays and disruptions in our scheduled work caused by a change in PI and the need to rebuild equipment. The older equipment was not suitable for methane hydrate work. We have built a new system and have completed pressure tests on the newly built system. Thus, we anticipate making our measurements on methane hydrates in the coming months.

8. Special Reporting Requirements

None

9. Budgetary Information

Attached separately